Energy 238 (2022) 121681

Contents lists available at ScienceDirect

Energy

journal homepage: www.elsevier.com/locate/energy

Energy assessment of an electrically heated catalyst in a hybrid RCCI truck

Antonio García, Javier Monsalve-Serrano*, Rafael Lago Sari, Santiago Martinez-Boggio

CMT - Motores Térmicos, Universitat Politècnica de València, Camino de Vera s/n, 46022, Valencia, Spain

ARTICLE INFO

Article history:
Received 14 April 2021
Received in revised form
29 June 2021
Accepted 2 August 2021
Available online 4 August 2021

Keywords:
RCCI
DOC
e-components
Full hybrid
Plug-in hybrid

ABSTRACT

Reactivity controlled compression ignition (RCCI) combustion showed great advantages in terms of engine-out NOx and soot emissions reduction. However, HC and CO emissions are larger than with conventional diesel combustion. Commercial oxidation catalysts can deal with the amount of HC and CO generated during the RCCI combustion only at warm conditions, thus limiting the implementation of this concept in conventional vehicles and in RCCI hybrid applications due to the large engine stop periods. This work aims to study the behaviour of an electrically heated catalyst used in a hybrid medium-duty truck operating with diesel-gasoline RCCI combustion. A parallel P2 full hybrid medium-duty truck is studied in transient conditions by means of numerical simulations validated with experimental data. The results are compared to those from the commercial diesel non-hybrid truck and the RCCI non-hybrid concept with a commercial oxidation catalyst. The results show that the fuel consumption increases about 2 % in combined cycles and 5 % in urban cases with respect to the non-hybrid RCCI case with a commercial oxidation catalyst. Finally, it was found that the RCCI hybrid concept with the electrically heated catalyst allows to achieve the EUVI targets for all the pollutant emissions with CO_2 levels of 15 %.

1. Introduction

Nowadays, pure electric trucks are being investigated as a potential solution to decarbonize the transport sector. However, due to the poor charging infrastructure and battery range and safety issues seems to not be applied at large scale soon [1]. In the meanwhile, other solutions are necessary to reduce the truck emissions. One option as intermediate step is the hybridization of the current powertrain technologies [2]. One problem of the hybridization of compression ignition engines is the cost addition of the new electric components to the current expensive thermal engine and aftertreatment systems. For this reason, low temperature combustion (LTC) as reactivity-controlled compression ignition (RCCI) is being studied by several research groups [3–5]. This concept avoids the use of the particulate filter (PF) and selective catalytic reduction (SCR) systems due to the ultra-low NOx and soot emissions [6]. However, the oxidation catalyst (OC) needs to be equipped due to large HC and CO emissions given by the gasoline port fuel injection and the low in-cylinder temperatures [7]. In spite the OC being a low-cost component, it is necessary understand if the commercial system can be used, or a new design needs to be proposed. In addition, a hybrid powertrain behaviour increases the engine on-off times with respect to the commercial non-hybrid applications [8,9]. Therefore, the impact of the temperature oscillation is crucial for the HC and CO conversion in the OC.

In an LTC concept as RCCI in which the major ATS component is the OC, the efforts need to be concentrated in the catalyst warm up and chemistry conversion. To achieve good conversion efficiency, the catalyst temperature needs to be above the light-off temperature, i.e. the point where the catalyst reaches 50 % conversion efficiency, when the engine is on [10]. A potential active technology is the use of an electrically heated catalyst (EHC) into the vehicle exhaust system upstream of the OC [11]. The EHC structure is heated through an electrical resistive heating and transfers the heat to the gas flowing through the EHC. The warmed gas then flows through the main catalyst structure, thereby heating the main catalyst to reach its light-off temperature more quickly than if heated solely by the engine-out exhaust gas [12]. Horng et al. [13] compared various converter configurations with the EHC and main converter in the underbody location versus close-coupled location, as well as having the EHC close-coupled but the main converter in the underbody location. The results from this work show that the

* Corresponding author.
E-mail address: jamonse1@mot.upv.es (J. Monsalve-Serrano).

https://doi.org/10.1016/j.energy.2021.121681

most effective strategy is to use the EHC plus main converter in the close-coupled location.

For HEVs, the well-studied fuel economy optimization approaches will usually implement frequent engine starts/stops, which can significantly impact the catalyst temperatures and performance [14]. The correct approach is to simultaneously optimize the fuel economy and reduce the tailpipe emissions for HEVs through the aftertreatment systems. To achieve this in an RCCI combustion, the attention needs to be concentrated in the light-off temperature strategy [15]. Different measures to reduce the OC light-off time in HEVs applications are the: close-coupled catalyst, exhaust gas temperature control and EHC. Exhaust gas temperature control is commonly performed by means of post injection strategies or increasing the engine load. The main disadvantage of both actions is the fuel consumption increase. An alternative is to use heating methods in the OC. Direct heating of the catalyst, where the catalyst substrate is used as a heating element, or indirect heating of the catalyst, where the heating element is placed upstream of the catalyst. The energy is coming from the battery that is recharged by regenerative braking or ICE charging mode. These charging methods lead to fuel penalties [16]. Therefore, the optimization of the heating method is crucial to reduce the CO_2 penalties. All these optimization tasks cannot be solved independently. Moreover, a unified framework is needed to deal with all the vehicle requirements and simultaneously satisfy constraints in terms of fuel economy, emissions, driveability, reliability and hardware costs.

This paper evaluates the application of an electrically heated catalyst on a hybrid medium-duty truck equipped with a RCCI engine. Using a 0D numerical model validated with experimental data, the effect of heating power on the light-off time and fuel penalty is determined. By means of a case study, the importance of an integral approach is explained. In this process, a mix of simulation and test data were combined, forming the foundations for future control developments of a suitable light-off strategy. Summarizing, the main contributions of this paper are: (i) development and experimental validation of a catalytic converter model for dual-fuel RCCI combustion and applied in a hybrid electric truck, (ii) investigating the impact of modifying the power input quantity for heating the ATS and the engine on-off times in the OC warm up speed, (iii) development of an RBC energy management strategy to minimize the fuel consumption and achieve the EUVI emissions targets at tailpipe conditions for all pollutants. To the best knowledge of the authors, no publications have concentrated so far on studying the simultaneous optimization of fuel consumption and tailpipe emissions in RCCI hybrid electric trucks.

2. Methodology

The methodology is divided in three parts: (i) vehicle model, (ii) oxidation catalyst model and (iii) case of study. The first topic describes the vehicle sub-models that allow to simulate the vehicle in steady-state and transient conditions. The second topic focuses on describing the OC and EHC model, and the control strategies used to reduce the light-off time. Lastly, a scheme of the proposed investigation with the different conditions where the vehicle is tested is presented.

2.1. Vehicle model

The 0-D vehicle model is implemented in GT-Suite commercial software (v2021, Gama Technology) for a medium-duty truck representative of the European goods delivery sector in urban areas [17]. Originally, the 18-ton (maximum payload) truck equips an 8L six-cylinder diesel engine (280 hp) with a six-gear manual transmission without any powertrain electrification [18]. The aftertreatment to achieve the EUVI limits is composed of a PF, OC, and SCR + ASC with urea injection. Nonetheless, previous results have demonstrated the capability of RCCI combustion in providing ultra-low NOx and soot [19]. Consequently, both aftertreatment system for these pollutants could be removed. In this sense, the present investigation assumes this scenario for NOx and soot and focus exclusively in the unburned products issues, that is one of the major drawbacks of the concept.

2.1.1. RCCI combustion and engine model

To promote the low temperature RCCI combustion, the ICE is modified and experimentally tested. The modification includes a new piston design, the addition of six port fuel injectors (PFI) to inject gasoline and the design of a new low-pressure exhaust gas recirculation (LP-EGR) line. The RCCI engine is evaluated through stationary tests in 36 operating conditions in the engine speed range of 950 rpm−2200 rpm and 10 %−100 % of engine load. A summary of the ICE modifications is depicted in Table 1 and the experimental test bed is showed in Fig. 1. The calibration is performed with the objective of achieving engine-out EUVI NOx levels (<0.40 g/kWh) and EUVI engine-out soot levels (<10 mg/kWh) with similar or better fuel consumption than CDC. As gasoline is injected in the PFI, large amount of HC and CO are emitted. Despite of considering the combustion efficiency improvement as a target to be optimized, the premixed nature of the combustion concept still implies an excessive quantity of HC and CO compared to that emitted by conventional engines.

The fully premixed combustion is achieved by setting the high reactivity fuel (HRF, diesel) injection early in the compression stroke [20]. The low reactivity fuel (LRF, gasoline) is injected in by means of a PFI at 340 CAD bTDC to promote a homogeneous mixture in the combustion chamber. The ratio of the gasoline mass over the total mass is referred to as gasoline fraction (GF, $m_{gasoline}/(m_{Diesel} + m_{gasoline})$). Fig. 2 shows the calibration maps for the RCCI concept. Specific species concentrations can be found also in Appendix, Figure A1 and Figure A2. The black dashed line marks the fully premixed limit, in which engine-out EUVI NOx and soot levels are achieved. To meet the CDC maximum brake power, a more diffusive combustion was promoted to reduce the in-cylinder peak pressure (zone between the black and red dashed lines). Therefore, the mentioned zone does not achieve engine-out EUVI soot emissions levels. To overcome this issue, it is proposed to de-rate the engine down to 14 bar of BMEP (brake power of 210 hp) for the hybrid powertrains. The lack of power of the RCCI de-rated ICE compared to the OEM diesel engine (280 hp) is compensated in the hybrid vehicle by means of an electric machine (EM).

Table 1
Main engine specifications for the CDC and RCCI engines.

Parameter	CDC ICE	RCCI ICE
Type	4 stoke, 4 valves	4 stoke, 4 valves
Nº Cylinders	6	6
Displaced Volume [cm^3]	7700	7700
Stroke [mm]	135	135
Bore [mm]	110	110
Injection type	DI diesel	DI diesel -PFI gasoline
Compression ratio [−]	17.5:1	12.8:1
High pressure EGR	Yes	Yes
Low pressure EGR	No	Yes
Turbo Configuration	VGT	VGT
Rated Power [hp]	282@2000 rpm	210@2200 rpm
Rated Torque [Nm]	1151@1500 rpm	858@1500 rpm
Aftertreatment [−]	OC + PF + SCR + ASC	OC

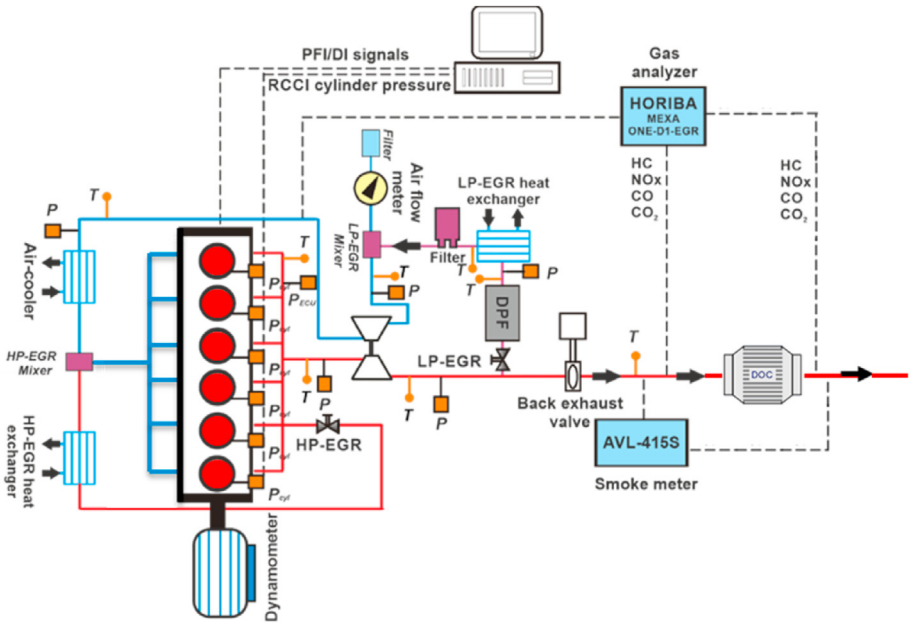

Fig. 1. Scheme of the engine test bed for an 8 L six-cylinder engine with the modification for operate in dual fuel mode.

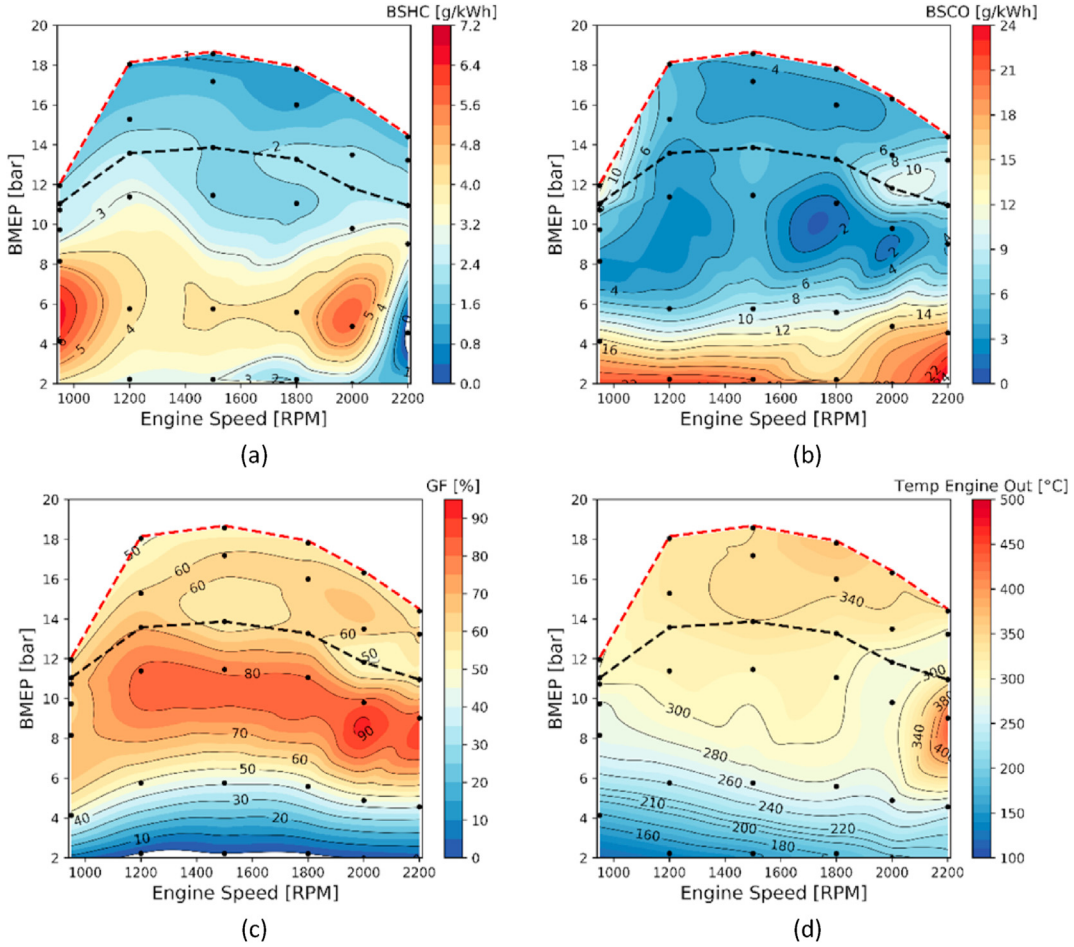

Fig. 2. Engine maps for the RCCI 8 L multi-cylinder ICE in terms of brake specific engine-out HC (a) and CO (b), Gasoline Fraction (c), and Exhaust temperature (d).

2.1.2. Hybrid powertrain model

The resistive forces (aerodynamic, friction, road slope, etc.) to model the truck platforms are obtained with road measurements of the commercial non-hybrid truck and depicted in Table 2. The validation of the vehicle model can be found in Ref. [21].

To assemble the hybrid powertrains, a battery pack and electric machines were added in the driveline. In this work a parallel P2 configuration is selected due to the small changes needed compared to the OEM truck [22]. In addition, this configuration allows the use of pure electric drive by decoupling the ICE by a second clutch system or boost mode by EM assist to the ICE. The proposed P2 RCCI hybrid truck is shown in Fig. 3. Moreover, a battery pack and all the power electronic systems with the inverter and signals conditioner are also added. It is important to note the addition of one extra fuel tank to feed the secondary injection system with gasoline fuel. To achieve the same maximum power than the non-hybrid version (280 hp), a 70 hp EM is added to compensate the 210 hp of the RCCI ICE. The gearbox, clutch 2 and final drive is maintained from the OEM powertrain architecture.

One important aspect in hybrid powertrains is the correct energy management system (EMS). There are several EMS that exploit heuristic or optimization-based methods [23]. The heuristic strategies typically rely on rule-based controllers (RBC) and load levelling logic, where usually no future driving information is needed. The results found in the bibliography show that the use of optimization-based strategies can improve up to 2 % the energy balance of the system (energy consumption) compared to that found with RBC. However, the application of these optimization-based strategies is not straightforward, being less robust and requiring higher computational resources. As studying different EMS is not the focus of this work, a previously calibrated RBC controller is used [21]. The novelty in this work is a calibration of the RBC including in the optimization loop the OC and EHC to improve the results is carried out.

The EMS with the RBC approach uses four control parameters to adjust the gear shift strategy in the automatic transmission, maximum vehicle speed where the truck leaves the pure electric mode and two parameters to control the battery charge strategy. In previous work [21] it was seen that the gear shift strategy is the most influence parameter in the fuel consumption because set the operative conditions zone in the engine map. Gear shift strategy at low engine revolution speed increase the ICE load, improving the brake thermal efficiency. However, a lack of power is seen when the truck is at high payload. Therefore, need to be find a balance between fuel economy and engine power available. In addition, the battery control is important for fuel economy and battery state of health. Both parameter (SOC start charge and SOC maximum charge) actuate in the ICE to start charging the battery and the charging, respectively. It is important to note that as it is a full hybrid truck, the target SOC will be the initial SOC when the driving cycle starts. If the actual SOC is equal to the set parameter, the ICE will deliver the maximum power. In mid-term cases, it is proportional to the target SOC. More information about the control strategy can be found in Ref. [8]. The optimum EMS calibration and components that were found in previous works [21] are depicted in Table 3. The optimum battery size was optimized between 8 kWh and 40 kWh for this truck. It is possible to see that the minimum value was selected. This is mainly because the fuel consumption improvements when the battery size increase (lower heat losses) it is lower than the increase in weight and total truck cost. This last parameter was analysed by a cost function that considers the European CO_2 penalties and battery cost [21]. The gear shift was tested between 1200 and 2200 rpm and the optimum was close to the minimum due to the increase in ICE efficiency with the reduction of the gear change speed. In addition, the pure electric mode of the truck change at low speed due to the type of combined driving cycle used for calibration. The battery control optimization was in the middle range tested. More information can be found in Ref. [21].

Table 2
Main vehicle specifications used as inputs in the 0-D truck models.

Base vehicle Mass [kg]	5240	Tires Size [mm/%/inch]	295/80/22.5
Max Payload [kg]	12760	Gear Box [−]	6 gears
Vehicle Drag Coefficient [−]	0.65	Differential ratio [−]	5.29
Frontal Area [m^2]	5.52	ICE rated power [hp]	280@2100 rpm
Rolling friction [−]	0.0155	ICE rated Torque [Nm]	1050

2.2. Oxidation catalyst model

This subsection aims to describe the modelling and validation process of the oxidation catalyst considering the 1D approach. Additionally, the simulation framework of the EHC is also discussed to stress the limitations and advantages of this approach. In an OC, the oxidation reactions of the carbon monoxide (CO), nitrogen oxide (NO) and total hydrocarbon (THC) emissions, only take place efficiently if the catalyst temperature is higher than the light-off temperature ($\approx$150 °C) [24]. This temperature is reached when the HC conversion achieves a 50 % efficiency. The time period that takes for the OC warmup up to this temperature is called light-off time. The complexity of the chemical reactions, the variation of the ICE engine-out conditions in a driving cycle and the thermal transient of the exhaust system makes this parameter extremely important in the powertrain development.

In this work, the ATS is proposed to use only the OC thanks to the pure RCCI engine operation. Two OC configurations are tested (Fig. 4), one equal to the OEM truck and other with a heater before the inlet of the OC with the aim to reduce the ATS light-off time and increase the HC and CO conversion efficiency.

More specifically, the electric heating is only applied to the first catalyst segment of the GT-Power model. This is a cost-effective solution where a relatively low heating power is required to reach the light-off temperature. Since only a small mass is heated, the catalyst reaches the light-off temperature very quickly. This enables a fast start of exothermal reactions (mainly from HC oxidation) to assist with the heating-up the remaining part of the catalyst. Note that the catalyst model includes energy balances for both the gaseous phase and the solid phase. These energy balances describe the heat transfer from convection, conduction and heat reaction.

2.2.1. Steady-state validation

First, the oxidation catalyst has been calibrated considering a dataset of experimental conditions as previously presented in García et al. [25]. The detailed modelling approach and data are described in previous works [26]. However, a brief description is herein provided. Fig. 5 depicts the GT-Power model that was built to calibrate the oxidation catalyst reactions using the Sampara et al. [10] mechanism. This model consists of two different parts. First, the geometric characteristics as wash coat width, length, channels density, presented in Table 4, are defined in the OC object while the chemical reactions from the chemical kinetic mechanism are specified in the reaction mechanism object. The specification of the concentration at the oxidation catalyst inlet was determined considering the approach proposed in Ref. [27], taking into account the most 11 representative species.

The global chemical kinetic mechanism requires a previous calibration using six operative conditions (Table 5) to obtain the Arrhenius parameters such as the activation energy and pre-exponential factor. The optimization process was performed using

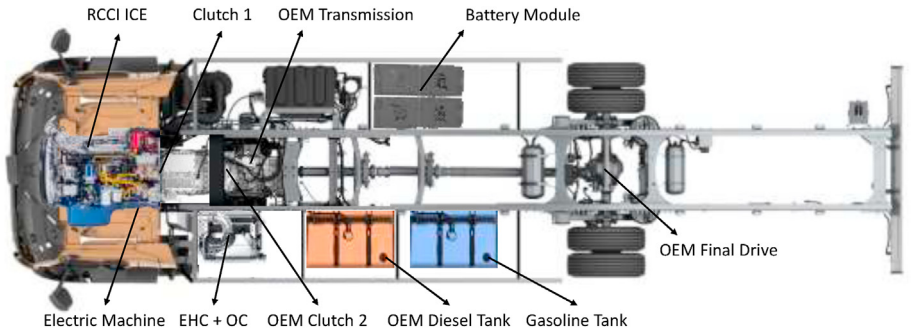

Fig. 3. P2 Hybrid architecture for the RCCI truck concept.

Table 3
DoE optimization parameters.

Parameter	Type of parameters	Range Tested
Battery Size	Hardware	8 kWh
Gear shift Strategy	Control Transmission	1370 RPM
Max Pure Electric mode	Control Electric machine	9 km/h
SOC start charge	Control Battery pack	0.49
SOC maximum charge	Control Battery pack	0.51

a genetic algorithm searching approach. Advanced techniques such as artificial neural networks and fuzzy-logic approach may be also enable a predictive description of the oxidation catalyst performance [28–30]. Nonetheless, they require larger datasets for calibration purposes compared with the physical based model used in this investigation. The results of the calibration and validation process are presented in Fig. 6. It is possible to see a good agreement between the predicted and experimental results of conversion efficiency for both HC and CO species. The higher deviations in CO conversion efficiency compared with HC are justified by the sensibility of this specie with the temperature. Additionally, the HC conversion efficiency is a consequence of both low reactivity and high reactivity hydrocarbon, enhancing the performance of the mechanism in harsh conditions. For additional details on the expected deviations and a detailed calibration description, please refer to Sampara and Bisset [10] and Garcia et al. [31]. The highest deviations are shown in temperatures lower than the light-off conditions. These conditions are generally representative of low load conditions, where the cyclic variability of the engine may produce a significant variation in the exhaust gas composition.

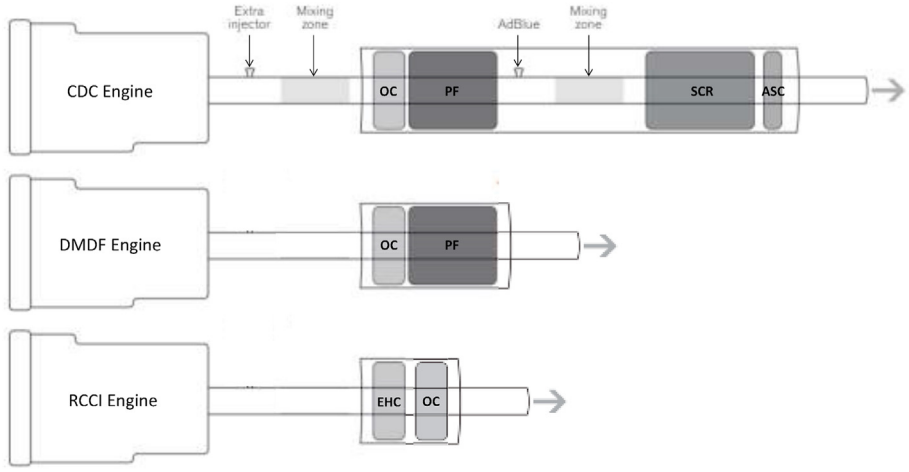

Fig. 4. Aftertreatment system scheme for the OEM diesel engine, DMDF non-hybrid and RCCI P2 hybrid powertrains.

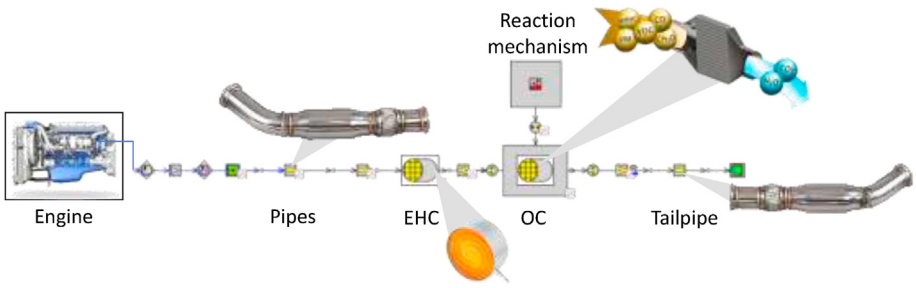

Fig. 5. GT-Power model for the Electrically Heated Catalyst (EHC) assessment.

Table 4
Geometric and components of the oxidation catalyst used in this investigation.

Volume	5.7
Diameter	10.5
Length	4
cpsi/mil	100/4
Substrate	Alumina
Washcoat	Cordierite

Despite the low deviation, the HC and CO emissions are slightly overestimated in the validation process for low temperatures. Therefore, this allows to use the model to be in the safe side to report the results.

2.2.2. Transient validation

In addition to the steady-state calibration, a further verification step was performed considering transient conditions. In this sense, the experimental results from previous experiments were used as boundary conditions to assess the capability of the model on reproducing the conversion efficiency of the experimental oxidation catalyst. The results of this evaluation for both HC and CO emissions are depicted in Fig. 7. As it is shown, it is possible to obtain a proper description of the conversion efficiency at transient operation at most of the time evaluated. The highest differences are evidenced at 400 s. This zone represents the time in which the engine speed is modified in the experiments, modifying not only the exhaust mass flow, but also the exhaust temperatures. Since the thermocouples are not designed to capture this thermal fast thermal transient, they may lead to a delay on the temperature reading, which is the main reason for the difference observed.

The delayed reading of the thermocouples can be observed in Fig. 8, where the simulated and experimental results of temperature are depicted. As it can be seen, the thermal model of the oxidation catalyst is able to describe the temperature variation at most of the transient step.

2.2.3. Modelling of the EHC

To reduce the tailpipe emissions levels, it is important to find an efficient thermal management strategy to quickly heat-up the aftertreatment device without hindering the benefits brought by the electrification. As the RCCI calibration has a high sensitivity to the injection strategy the use of delayed injections might be not the best strategy to increase the exhaust temperature. In this sense, other alternatives should be pursued. A fast catalyst heating offers an effective manner to minimize the catalyst light-off time and

Table 5
Operating points for the OC model calibration and validation.

Operating Point	Engine Speed	BMEP	Exhaust gas mass	Temperature engine-out	HC	CO	HC conv	CO conv
_	[rpm]	[bar]	[g/s]	[°C]	[ppm]	[ppm]	[%]	[%]
Cal 1	1200	2.15	43.5	176	432	2436	42.8	12.0
Cal 2	1200	5.66	57.5	256	3912	1420	96.5	99.9
Cal 3	1500	5.74	76.9	273	3432	1737	96.8	99.6
Cal 4	1800	2.10	75.7	208	742	1433	89.9	99.7
Cal 5	2000	1.91	81.0	214	720	1501	91.6	99.7
Cal 6	2200	1.78	85.3	227	329	2335	92.2	99.8
Val 1	1500	2.1	54.7	191	1599	2467	43.0	19.5
Val 2	2000	2.0	80.6	217	268	1781	87.3	99.8
Val 3	1200	5.6	59.1	282	3890	1118	98.0	99.8
Val 4	1800	5.4	91.4	287	3613	2108	97.1	99.7
Val 5	1500	7.8	76.2	287	977	1536	97.9	100.0
Val 6	2200	4.6	118.9	296	4054	2953	96.5	99.4
Val 7	2000	4.7	98.5	302	4482	2856	97.0	99.4
Val 8	2200	8.8	169.0	327	1606	1389	96.6	100
Val 9	2000	9.7	151.8	342	1404	952	97.7	100

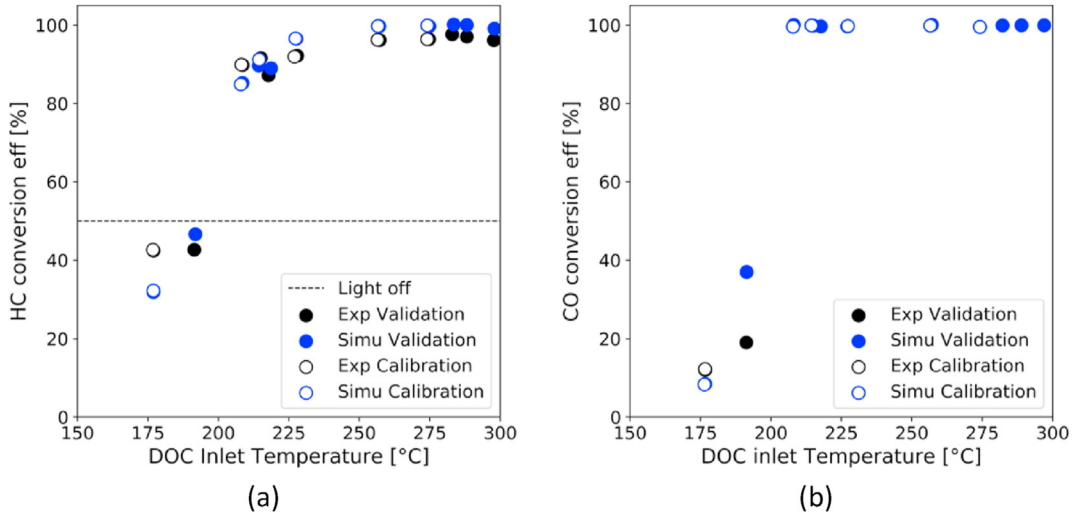

Fig. 6. Experimental versus simulated conversion efficiencies for (a) unburned hydrocarbon and (b) carbon monoxide considering the calibration and validation operating points.

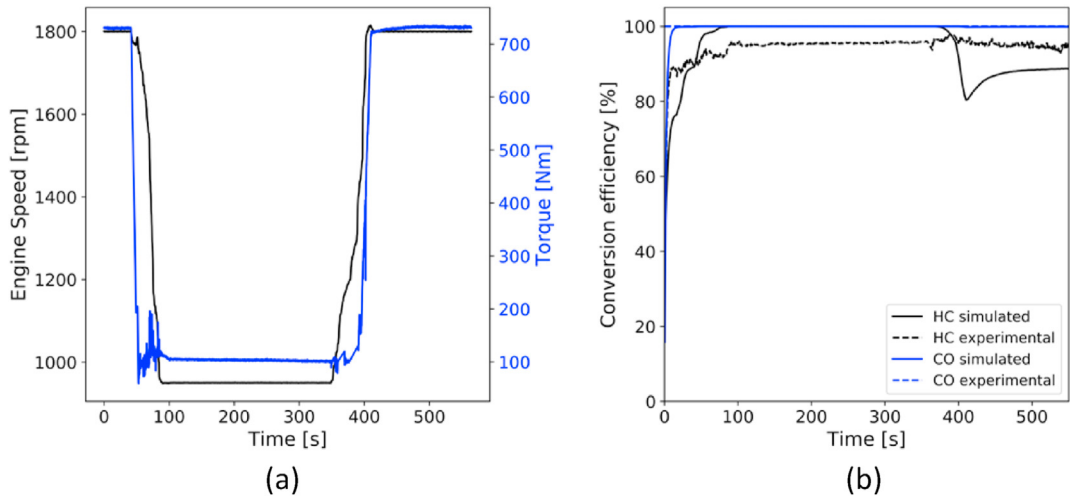

Fig. 7. Engine speed and engine torque to evaluate experimental and simulated conversion efficiency (a). Comparison between experimental and simulated conversion efficiency for unburned hydrocarbons (black) and carbon monoxide (blue) (b). (For interpretation of the references to colour in this figure legend, the reader is referred to the Web version of this article.)

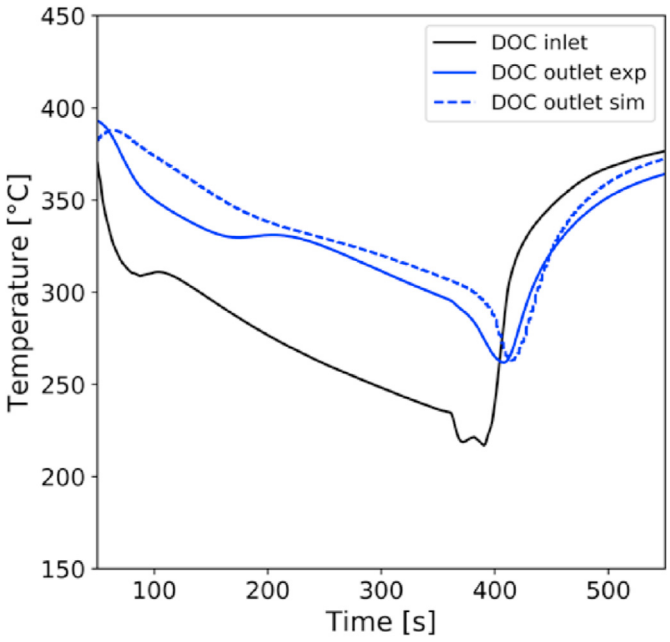

Fig. 8. Inlet temperature and comparison between experimental and simulated temperature results at the DOC outlet.

hence, reduce the exhaust emissions from the start-stop events. On the other hand, offering additional heat to the catalyst leads to more energy consumption, which typically results in additional fuel consumption. Various control strategies exist for the catalyst heating as pre-heating and post-heating. As the control system is not predictive in terms of engine use and vehicle future speed (which is required for pre-heating strategies), only post-heating was used in this work.

As previously introduced, an EHC consist of an electrical resistance which provides energy to the flow at the cost of an electrical consumption. The efficiency on transferring the energy to the flow is proportional to the residence time of the flow inside the EHC and the contact area. Both are directly influenced by geometric parameters of the EHC such as length and porosity. In this study, these parameters were obtained by having as reference the EHC model proposed by Della Torre [32] for light-duty vehicles and scaling it considering the OC diameter as reference. The final model of the EHC coupled with the OC is presented in Fig. 5. The EHC is located just in front of the OC, with a length equal to the 25 % of the OC length and the same diameter, and the same substrate geometry (cell density and wall thickness). The heat is delivered to an iron mesh where the exhaust gas is heated-up by convection. A 94 % of conversion efficiency is set for the passage from electricity to heat power follow the measurements found in Ref. [33].

The EHC is connected to the 600 V battery system by a DC/DC converter to feed the 48 V EHC system. Therefore, the energy consumption is directly seen in the battery SOC and it will impact the total fuel consumption. The numerical model includes all the electrical losses as well as the battery cell limits. It is important to note that the cases with EHC will have a dual effect: 1) CO and HC tailpipe emissions levels will decrease due to the high OC temperature, 2) CO and HC engine-out emissions levels will increase due to the higher fuel consumption. The results will contemplate the impact due to the connection of the EHC electric system to the battery. The EHC operation was set to be on when the ICE is also running and the OC wall temperature is below 150 °C, as shown in the example of Fig. 9.

2.3. Case of study

To understand the HC and CO conversion in the oxidation catalyst for different EHC heat addition and engine operation conditions, a simplified model with the ICE and OC was built. This allows to operate in a steady-state ICE operative condition (fixed engine-out temperature, mass flow and emissions composition) while observing the OC warm up and the conversion behaviour. Since the exhaust gas temperature will have an impact in the OC performance, it was studied the same mass flow and gas compositions of the experimental measurements (steady-state) but with 25 °C and 50 °C less temperature. In addition, the effect of the EHC heat source and the amount of on-off ICE times were also explored by means of parametric studies. This type of analysis will be impossible on a real ICE test bed and will be costly in time and money on an ATS test bench. Therefore, it was proposed as first step in the results section to well understand the OC and EHC performance under controlled conditions.

A further evaluation step consists of the ICE and OC transient

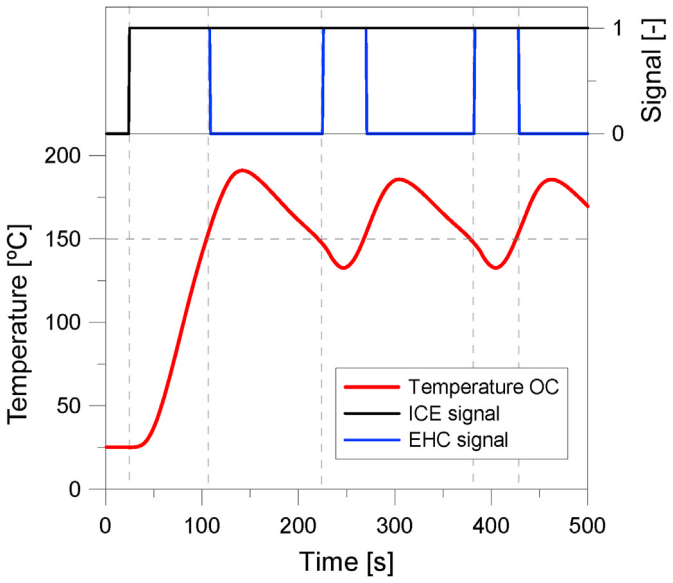

Fig. 9. EHC post-heating scheme with the EHC signal in terms of engine on-off signal and OC wall temperature.

study. The previous powertrain calibration without considering the OC operation was studied as first case. The World Harmonized Vehicle Cycle (WHVC, Figure A4a) at 50 % payload is used as representative of the European homologation for heavy-duty trucks. The use of the EHC is compared against the case without the heater. Later, to improve the results, a new calibration was performed by means of a design of experiments (DoE) including the OC and the EHC in the optimization loop. Lastly, the optimum case is studied in different driving cycles (see Figure A4) that represent real driving patterns obtained with the SUMO software for Paris (see Figure A3).

3. Results

3.1. Steady-state operation

The first step was to study the heat addition influence in the OC wall temperature on the HC and CO conversion efficiency. Four cases ranging from 0 kW to 10 kW were tested in an engine operating condition selected as critical. The selected point is 1200 rpm and 6 bar of BMEP, which is widely used in hybrid operation (see previous work [21]) and both the amount of HC are large (4 g/kWh) and the engine-out temperature is low (210 °C) for a medium load point.

Fig. 10a show the increase in the OC wall temperature during the warm-up and the impact on the HC conversion (Fig. 10b) with the heat addition. The impact in the final tailpipe HC emissions is shown in Fig. 10c, with a decrease of 40 % between the extreme cases. The derivate of the HC emissions after the OC shows that for this operative condition, 5 kW represents the optimum scenario. Therefore, it will be adopted as a proper heating rate in the next EHC simulations. Despite other operating conditions can show a different optimum heat addition, the determination of each optimum is not the focus of the current manuscript.

As explained in the previous section, 36 ICE operating conditions (950–2200 rpm of engine speed and 2–18 bars of BMEP) in RCCI combustion mode were studied with the OC starting from ambient temperature. Fig. 11 shows the light-off time (time required to achieve 50 % of HC conversion in the OC) for three ICE engine-out temperatures. Fig. 11a show the effect of steady-state temperature presented as an interpolate map of all the operating conditions. The light-off time only takes more than 20 s for low engine speed and load. At medium engine speed and load, where the RCCI low temperature combustion uses the highest gasoline fraction (see Fig. 1), the OC takes around 10 s to achieve the light-off temperature. For higher loads and engine speed, the time is highly reduced. Fig. 11b and c shows the effect of the temperature decrease from the engine-out up to the OC inlet due to heat transfer. Since this temperature decrease depends on several factor as pipe length, thermal insulation, etc, a parametric study was proposed consisting of using two different temperature levels: 25 °C and 50 °C less temperature, respectively. From the results, it is possible to observe that the light-off time highly increases in low engine speeds. The case of 950 rpm and 4 bar BMEP cannot achieve the light-off temperature. At the case of 50 °C less than steady-state temperature, the central region of the map doubles the time to achieve the light-off temperature.

To reduce the above-mentioned time, the addition of a heater before the OC can be considered a potential solution. Fig. 12 shows the light-off time when 5 kW of heat is applied in the EHC for the three engine-out temperature conditions. Using the same colour scale than Fig. 11, the map is converted all in blue. This means that the light-the light off temperature is achieved in all conditions and not surpass the 10 s for any case.

Despite the light-off being an important condition for reference to compare with other works, due to the amount of HC and CO emitted in the RCCI combustion, high conversion efficiencies (above 90 %) need to be achieved. Fig. 13 shows the OC wall temperature and HC conversion efficiency at 1200 rpm and 6 bar BMEP. The EHC has a strong effect on the OC temperature. The condition of cold engine-out gas temperature (steady-state less 50 °C) is faster than the steady-state condition without the heater. This is an important point for the RCCI combustion during the first seconds of the engine warm-up. This is a critical aspect of the low temperature combustion application, since it combines low exhaust temperatures with excessive unburned products concentration.

To study the ICE engine on/off effect in controlled conditions, results from previous works [21], it is possible to obtain the necessary brake energy delivered by the engine in a driving cycle (WHVC) and payload (50 %) condition. The steps are created and shown in Fig. 14 based in the operative condition of 1200 rpm and 6 bar BMEP. It is important to note that the total time of the engine in on mode is independent of the start and stops times ($ICE_{on\_off\ times}$). However, the split is crucial for the OC temperature.

The duration (ICE_{ontime}) on the driving cycle can be obtained following the equation:

$$ICE_{on\ time}[s] = \frac{E_{cycle}\ [kWh]}{Power_{ICE}\ [kW]} \frac{3600}{ICE_{on\_off\ times}[-]} \quad (1)$$

$$ICE_{off\ time}[s] = \frac{Total\ Time_{cycle}[s]}{ICE_{on\_off\ times}[-]} - ICE_{on\ time}[s] \quad (2)$$

with $Power_{ICE}$ as the power delivered at the selected operative condition and the $TotalTime_{cycle}$ is 1800 s for the WHVC. In this study, a parametric analysis of the number of starts in the driving cycle ($ICE_{on\_offtimes}$) is done. In addition, the use of the EHC was accomplished with 5 kW delivered if the engine is on and the OC wall temperature is below 150 °C. Fig. 15a show the effect of the engine starts in the HC emissions. For both cases exist an intermediate case where the EUVI limits are not met. In the case of CO (Fig. 15b), the legislation limits are achieved for all the cases due to the lower CO emissions and more flexible requirement than HC. The behaviour of this last pollutant can be explained with the OC

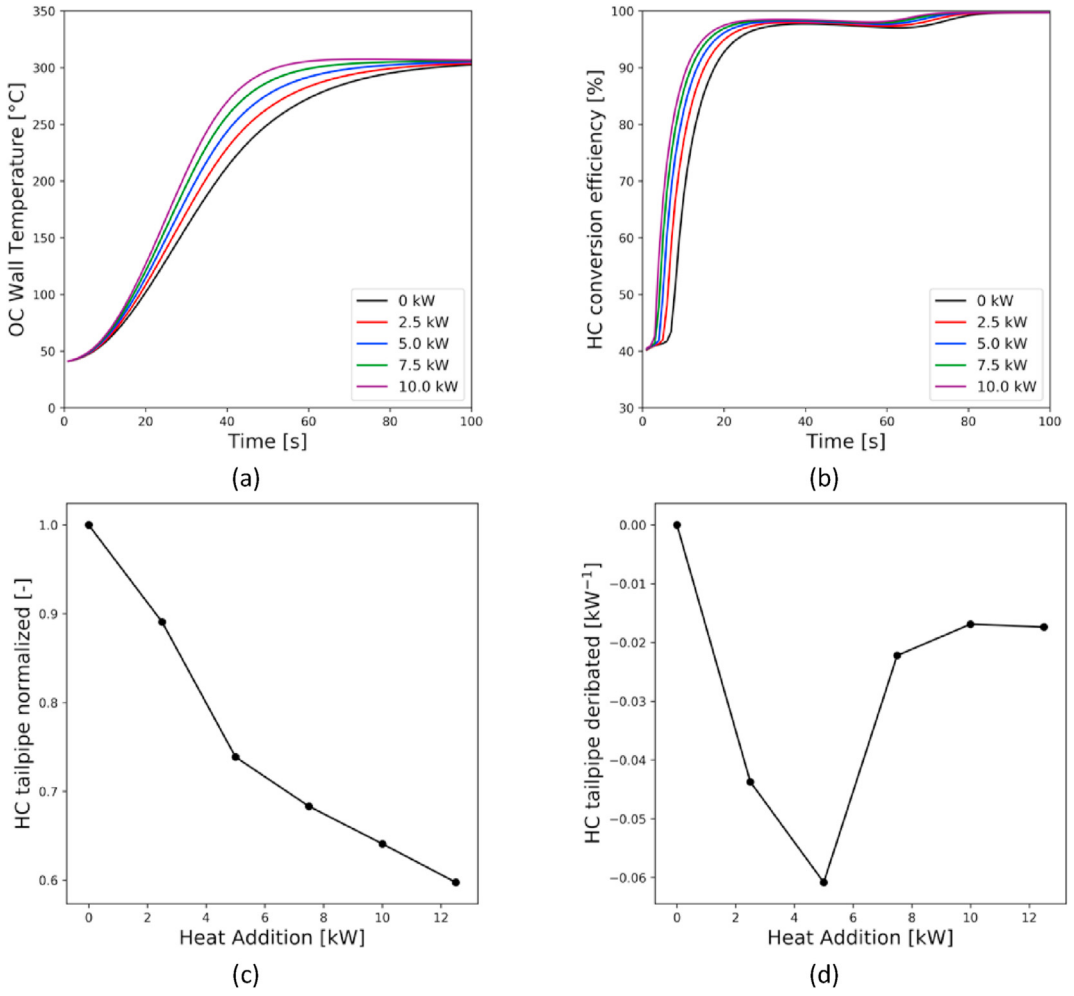

Fig. 10. Heat addition effects at 1200 rpm and 6 bar BMEP on the HC tailpipe emissions normalized EUVI (a) and derivate HC tailpipe emissions normalized (b) with heat addition.

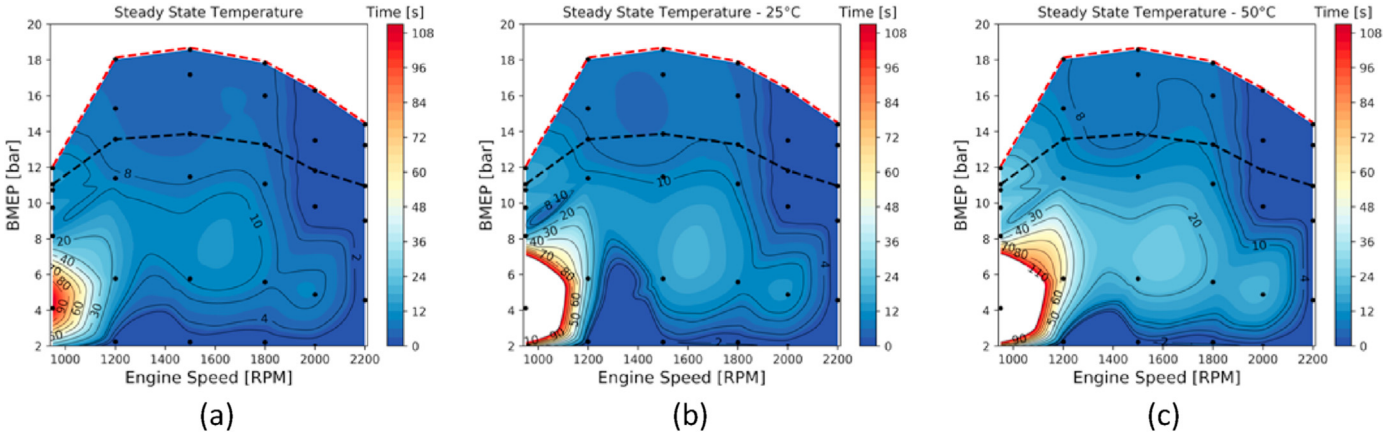

Fig. 11. Light-off time map for three engine-out temperatures: steady state (a), steady state minus 25 °C and (c) steady state minus 50 °C without EHC.

wall temperature when the engine is on. In spite of that the average temperature of the OC decreases with the number of starts (Fig. 15c), the standard deviation has an increase and then decrease with the number of starts as the HC emissions. This last parameter is crucial because the OC conversion does not improve by increasing the temperature only, the main point is being above the light-of temperature ($\approx$150 °C) most of the time.

To give more insights in this point, Fig. 16 shows a kernel density estimation approach was performed to obtain insights about the distribution of the temperature during the OC operation. In addition, the best fitting Gaussian curve was added to the graph, allowing to stress the effect of the number of ICE starts on the OC wall temperature. It is interesting to see that the increase of the ICE starts does not necessarily increase the OC operation. As it can be

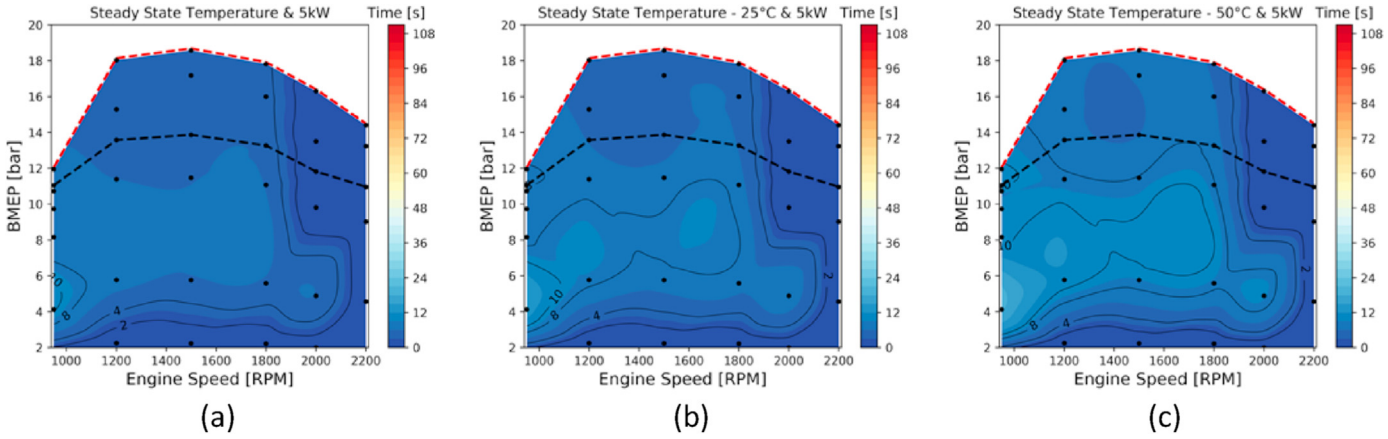

Fig. 12. Light-off time map for three engine-out temperatures: steady state (a), steady state minus 25 °C and (c) steady state minus 50 °C with 5 kW in the EHC.

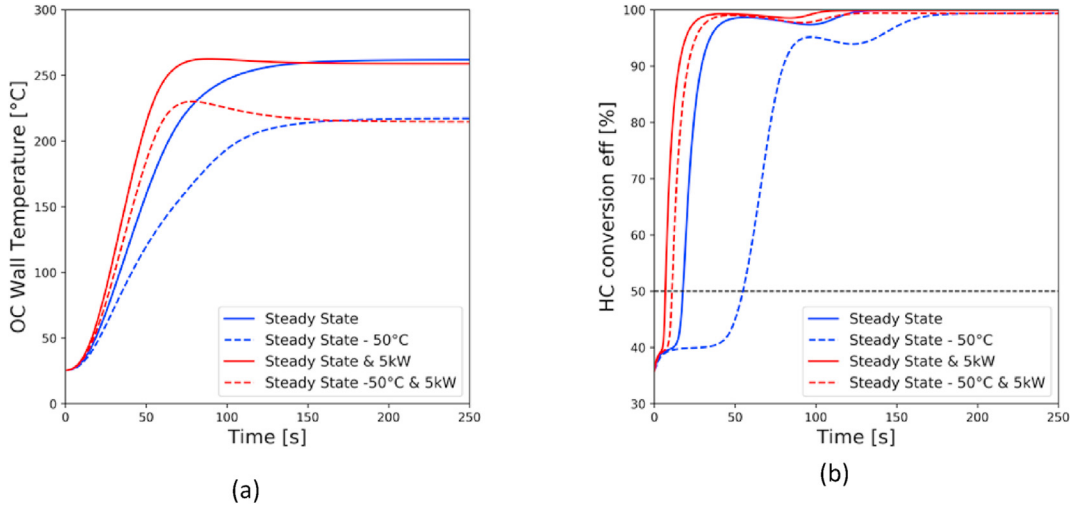

Fig. 13. OC wall temperature (a) and HC conversion efficiency (b) for steady-state temperature and the steady-state temperature minus 50 °C with and without EHC at 1200 rpm and 6 bar BMEP.

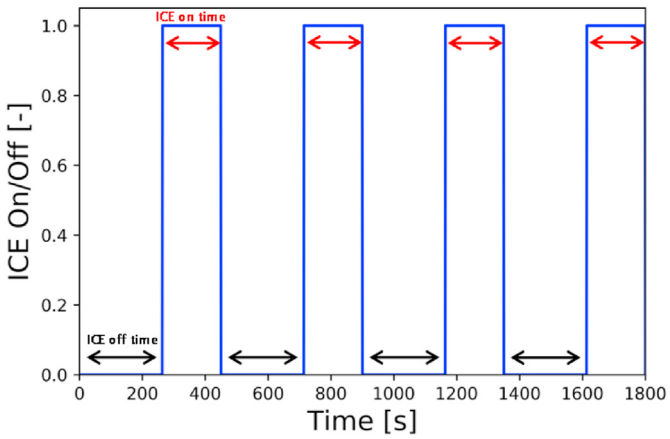

Fig. 14. Diagram of the ICE starts (example of 4 starts) in the same steady-state point for the WHVC (1800 s).

seen in Figs. 15 and 1 start means that once the OC achieves the light-off operation it remains at very high temperature during most of the operation, assuring a good conversion efficiency. Nonetheless, for 8 ICE starts, the wall temperature is decreased always as the ICE is turn-off. This means that the temperature distribution is wider and also achieves lower values, impairing the conversion efficiency. In the case of 20 ICE starts, the average temperature is not too high, but it is concentrated above 150 °C, which is a proper temperature range for the OC operation.

3.2. Transient operation

After the detailed analysis with the ICE working in steady-state conditions and the OC warm-up behaviour, the next step is the study in real vehicle operation. To do this, the P2 hybrid truck operating in the homologation driving cycle WHVC with different payloads is modelled. Fig. 17a show the engine on-off states when 50 % of payload is applied. This case represents the optimum calibrated case to fulfil the EUVI NOx and soot emissions at engine-out conditions with the lowest CO_2 emissions. This case is extracted from a previous work of the research group [21]. The number of starts for the optimum was 12 starts, between the range of the steady state study (1–20 starts). The optimization not considered the HC and CO emissions. Therefore, the number of starts was optimized to achieve the minimum fuel consumption. It is interesting to remark that the addition of the chemistry simulation in

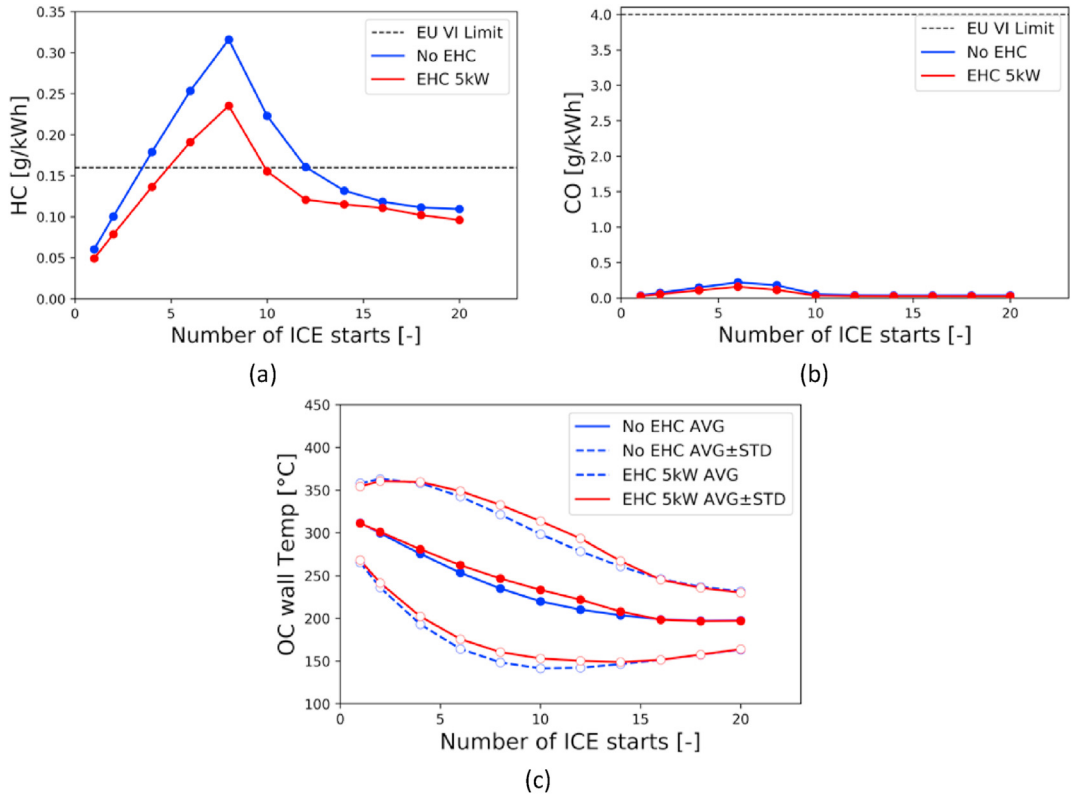

Fig. 15. HC (a), CO (b) emissions after the OC and OC wall temperature (c) against the number of ICE starts.

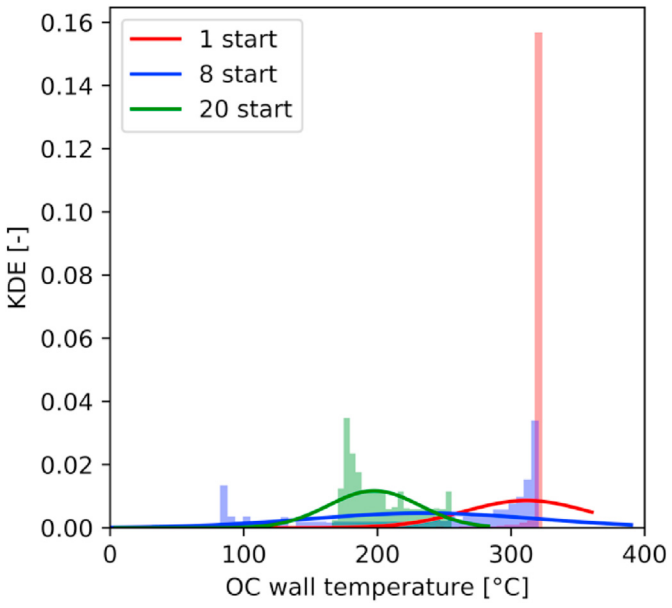

Fig. 16. OC wall temperature distribution for the extreme ICE starts cases and the worst case in terms of HC emissions.

the catalyst has significantly increased the computational time from 0.1 to 4 times the real time.

Fig. 17b shows the HC emissions before and after the OC. The first 600 s are responsible for the large amount of HC emissions. This is a direct consequence of the low OC temperature, depicted in Fig. 18. The amount of ICE-off time due to the urban phase makes the case without the heater to produce 70 % of the total HC emissions. When the EHC is added with 5 kW under the same calibration of the case without EHC, the HC emissions are strongly reduced. It is possible to achieve the EUVI legislation due to the fast increase of the OC wall temperature. For both cases, the EUVI CO targets can be easily achieved. Therefore, it can be concluded that one of the main limits to implement the RCCI combustion with hybrid architectures are the HC emissions.

However, the use of the EHC has an impact on the final fuel consumption/CO_2 emissions. Table 6 shows that, in average, the use of the heater with 5 kW increases the CO_2 emissions by 1.0 % with respect to the case without the EHC. The advantage of the EHC is that it allows to achieve the EUVI limits for all the emissions (NOx, soot, CO and HC) for the homologation case, while still providing a CO_2 reduction of 15.7 % (the European target for 2025 is to achieve 15 % of CO_2 reduction for heavy-duty transportation with respect to 2020). It is important to note that the empty truck conditions (0 % payload) are the worst scenario due to the low energy requirement. From a previous study of the research group [31], it was shown that the non-hybrid version does not achieve the EUVI HC limits under empty cargo due to the operation only at low BMEP conditions. The hybridization enables improvements of this scenario with respect to the non-hybrid case since it allows to use the ICE at high engine loads. However, without a dedicated calibration to reduce the ICE on-off times, the HC limit is not achieved for 0 % of payload even with the use of an EHC, as shown in Table 6.

In this sense, a DoE with all the hybrid calibration parameters (Table 3) is performed including the OC in the simulation. Differently from the previous results, a controller for the ICE on-off time is added. This control forces the ICE to maintain at the same state condition for a set time reducing the number of on-off events. However, this time cannot be always achieved due to the small electric machine (ratio of hybridization is 25 %) and battery package (8 kWh, 5 % of an equivalent pure electric truck) that is used. When

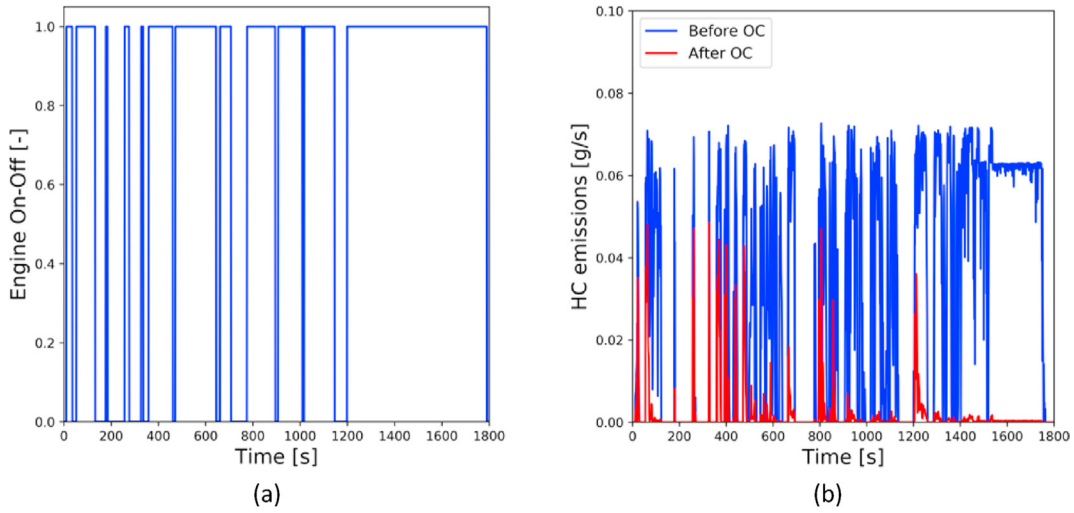

Fig. 17. Engine on-off (a) and HC emissions before/after the OC (b) for the WHVC with 50 % payload in a RCCI P2 hybrid Truck without EHC.

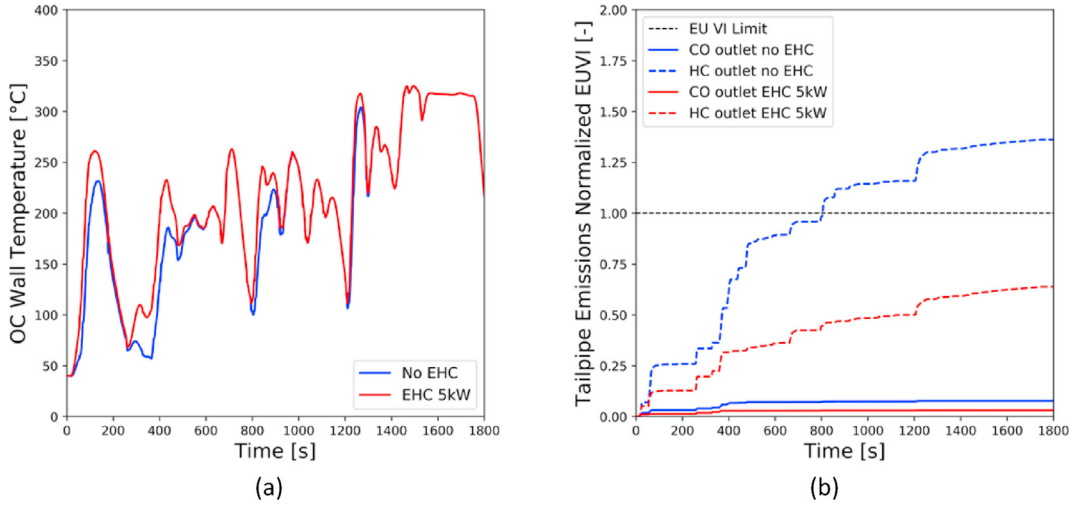

Fig. 18. OC wall temperature (a) and HC and CO normalized emissions with respect to EUVI (b) for the WHVC with 50 % payload in a RCCI P2 hybrid truck without and with the EHC.

Table 6
Summary of the main parameters for the RCCI P2 hybrid truck without and with the EHC in the WHVC with different payloads.

Case	Tailpipe CO_2 emissions vs CDC non-hybrid	HC emissions [g/kWh]	CO emissions [g/kWh]
0 %	−19.6 %	0.66	2.34
0 % EHC	−17.9 %	0.20	0.27
50 %	−16.2 %	0.19	0.27
50 % EHC	−15.7 %	0.09	0.11
100 %	−9.5 %	0.10	0.17
100 % EHC	−8.6 %	0.06	0.10

*Red colour means values out EUVI limit or below 2025 European CO_2 target.

the desired wheel torque is higher than the EM maximum torque or the battery is full or depleted, the ICE will change the state without following the on-off minimum time rule. In any case, this parameter helps to control the ICE behaviour.

Fig. 19 shows the new calibration results in terms of HC tailpipe emissions (after the OC) versus the ICE start times and the ICE control parameter for both cases, with and without the EHC. The new calibration allows to achieve the EUVI HC limit by reducing the number of engines starts also in the case without the EHC. Despite the ICE minimum time helps to decrease the number of engines starts, after 100 s (transition from red to blue colour bar) the effect is null due to driving cycle requirements for this payload condition. The range of starts was between 6 and 22, and the best cases were achieved below 10 starts. This cannot be directly linked to the analysis of Fig. 15 due to the difference of the transient conditions (different operating points). However, it can be qualitative compared. It is seen that reducing the number of starts reduces the HC tailpipe emissions as the case of the steps. However, the main difference is that the further increase of the number of starts from 20 does not improve the results compared to the steps case (Fig. 15).

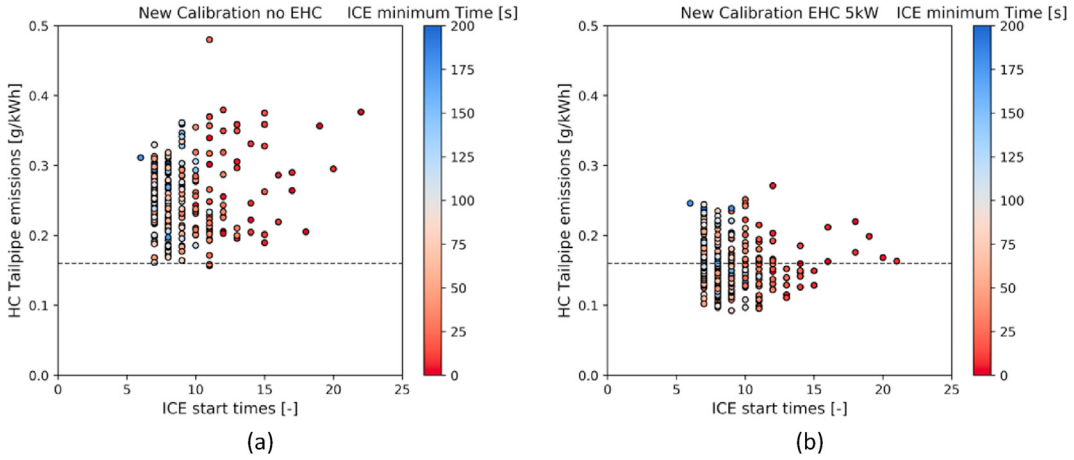

Fig. 19. HC tailpipe emissions (after the OC) against the ICE start times and ICE minimum time control for the new calibration without EHC (a) and with EHC 5 kW (b).

Therefore, increase the control time to reduce the number of starts is the best option in real transient conditions.

Fig. 20 shows that the CO_2 tailpipe emissions increases by reducing the ICE starts and the use of the EHC. Both strategies reduce the improvements with respect to the baseline case around 1.25 % the CO_2 emissions. Therefore, if both strategies are applied the penalties achieves the 2.5 % of CO_2 reduction. However, the EHC impact allows to not need the high reduction of ICE starts. The case of lowest CO_2 emissions and HC and CO under EUVI limits differs only in 0.7 % CO_2 penalty. To summarize, Table 7 shows the effect of both controlling the ICE on-off times and using the EHC in other payloads. For the most challenging condition (0 % payload), the new calibration allows to achieve the EU VI limits. These results suggest that a hybrid RCCI truck can achieve the EUVI limits for all the emissions under homologation conditions for the entire range of payloads with the OEM OC and an EHC with 5 kW of heat addition with a dedicated controller.

The benefits in a cycle that combines urban, rural and highway route with the re-calibration and use of the EHC shows great improvements. However, the question is if it will behave similar in pure urban cases. Therefore, 3 cycles performed with SUMO tool in Paris city centre was generated. These routes are representative of truck routes with a duration of 2000 s for the first two cases and 4000 s for the third case. Fig. 21a show the OC wall temperature for the case of the non-hybrid DMDF truck, P2 hybrid with the new calibration for both cases, with/without EHC. The non-hybrid maintains a higher mean temperature due to the absence of ICE on/off but the maximum temperature is always below P2 hybrid due to the low engine load operation. The case of EHC increase the temperature with respect to the no EHC case almost all the driving cycle. Fig. 21b shows the cumulative HC and CO emissions normalized with respect to EUVI limits in the first SUMO cycle with 0 % payload (most challenge case). The hybrid powertrain improves the HC and CO emissions by far due to the better ICE use (operative conditions with higher brake thermal efficiency). However, for the case of HC tailpipe emissions it is not possible to achieve EUVI due

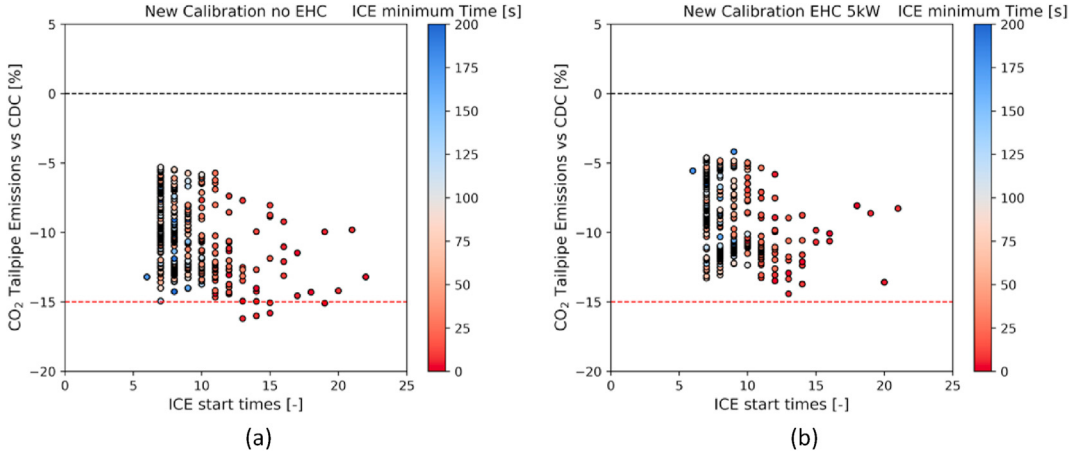

Fig. 20. Fuel consumption against the ICE start times and ICE minimum time control for the new calibration without EHC (a) and with EHC 5 kW (b).

Table 7
Summary of the main parameters for the RCCI P2 hybrid Truck without and with EHC in the WHVC with different payloads with a new dedicated OC calibration.

Case	Tailpipe CO_2 emissions vs CDC non-hybrid	HC emissions [g/kWh]	CO emissions [g/kWh]
0 % New cal	−16.5 %	**0.33**	0.39
0 % EHC New cal	−18.4 %	0.14	0.30=
50 % New cal	−15.1 %	0.16	0.22
50 % EHC New cal	−14.4 %	0.10	0.20
100 % New cal	−9.6 %	0.09	0.10
100 % EHC New cal	−8.6 %	0.07	0.09

*Red colour means values out EUVI limit or below 2025 European CO_2 target.

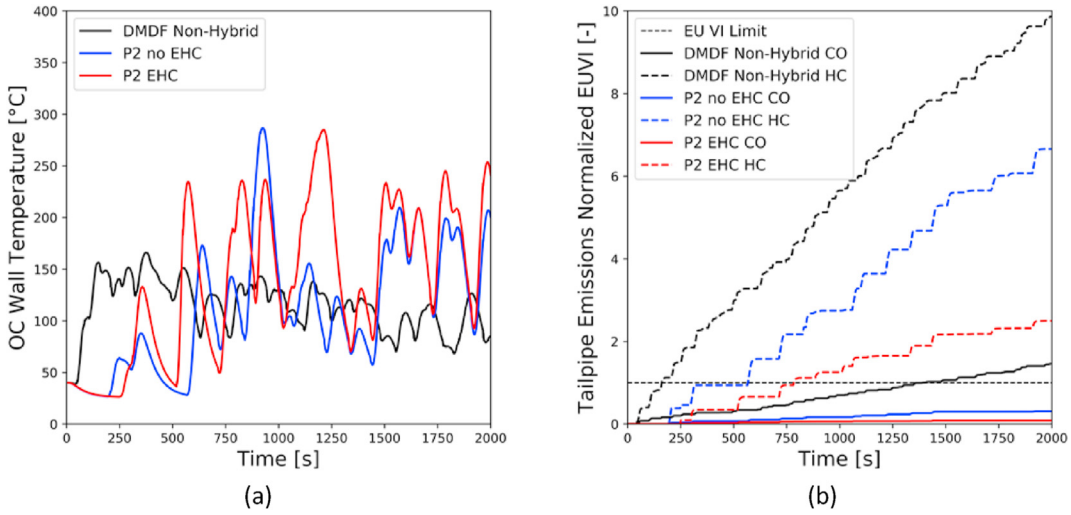

Fig. 21. SUMO 1 driving cycle under 0 % Payload for OC wall temperature (a) and HC and CO tailpipe emissions normalized to EUVI for DMDF non-hybrid, P2 hybrid with the new calibration with/without EHC.

to the large amount of start and stops of the vehicle. The OC temperature has minimum of 50 °C several times during the cycle.

A summary of all cases is shown in Fig. 22. The HC and CO emissions are presented in absolute values and marked with dashed ball when achieves EUVI emissions (CO = 4 g/kWh and HC = 0.16 g/kWh). It is possible to observe a strong improvement with respect to DMDF non-hybrid due to the right hybrid powertrain calibration. However, 0 % and 50 % of payload in urban cases are challenging conditions for EUVI achievement. The SUMO 3 that increase the cycle time and has a last phase of rural allows to achieve EUVI in all conditions for the hybrid powertrain. The EHC improves the tailpipe emissions with cases of 3 times of reduction with respect to P2 without EHC. Lastly, CO_2 emissions with respect to the current CDC non-hybrid commercial truck shows that 2025 CO_2 targets in urban cases is easily to achieve for the P2 hybrid powertrain. Low payload also allows to achieve 2030 CO_2 target (30 % of CO2 reduction). The use of EHC penalize the CO_2 emissions by an average of 2 %. For the four cycles and three payloads the average gains for the hybrid operation was 21.3 % without EHC and 19.3 % for the case of EHC. The non-hybrid DMDF increase the CO_2 in 0.8 % with respect to the diesel case.

4. Conclusion

A deep study of the oxidation catalyst behaviour in a hybrid RCCI medium-duty truck was performed using experimental and numerical tools. The addition of an electrical heater at the inlet of the OC was included in the analysis. The main findings of the study are listed below:

- The experimental validation demonstrates that the 1D OC numerical model can predict the HC and CO conversion with high accuracy at stationary and transient conditions.
- The stationary ICE analysis allows to select the best EHC heat addition (5 kW), to demonstrate the effect of the ICE engine-out temperature and to show the ICE on-off effect in the tailpipe emissions. Up to 50 °C lower engine-out temperature, the EHC allows to minimize the light-off time impact. In addition, the ICE engine-off time analysis shows that it is important to reduce the ICE state changing period.
- Considering the driving cycle assessment of the hybrid architecture, the calibration without accounting for the HC emissions shows that only at 100 % payload it is possible to achieve the

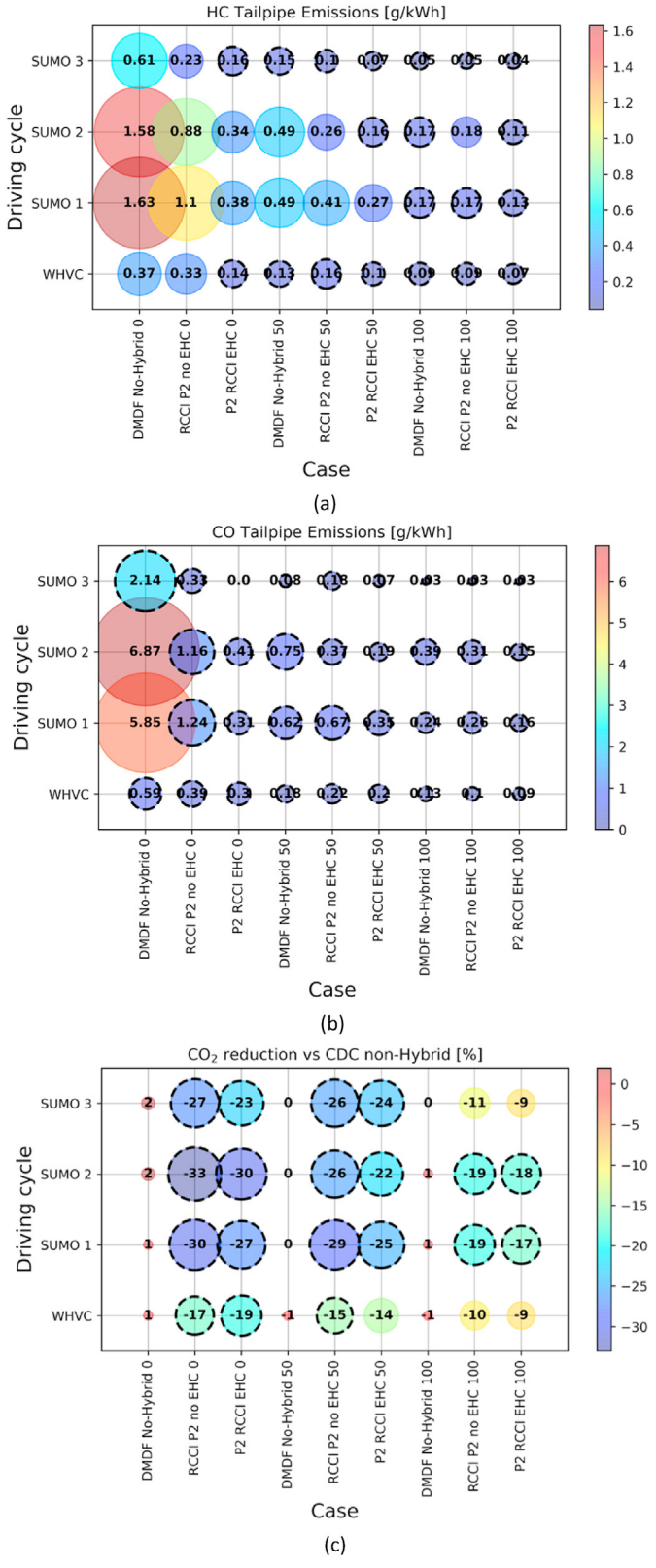

Fig. 22. All driving conditions HC tailpipe emissions (a) CO tailpipe emissions (b) and CO2 tailpipe reduction compared with CDC non-hybrid (c) for DMDF non-hybrid, P2 hybrid with the new calibration with/without EHC.

EUVI limits. When the EHC is added, 50 % payload (homologation case) also presents the EUVI compliant values.

- The re-calibration using an additional state control in the ICE minimum on-off time allows to achieve the EUVI limits in all conditions except for 0 % payload. Here, the addition of the EHC enables to achieve the EUVI limits to with the empty truck.
- Lastly, the real driving cycles shows that urban cycles benefit the CO2 reduction with gains of 30 % in low payloads and above 15 % in full payload. However, the HC emissions are a challenge. Low payload cannot achieve EUVI also with the re-calibration and EHC. In spite of the difficulties, the EHC largely reduce the HC and CO emissions.

In future works, the numerical calibration obtained will be tested in the experimental ICE test bed to further study the emissions composition, ICE engine-out temperature and the EHC behaviour.

Credit roles

Antonio García: Conceptualization; Javier Monsalve-Serrano: Writing – review & editing; Rafael Lago Sari: Methodology; Santiago Martínez-Boggio: Writing – original draft.

Declaration of competing interest

The authors declare that they have no known competing financial interests or personal relationships that could have appeared to influence the work reported in this paper.

Acknowledgments

The authors thanks ARAMCO Overseas Company and VOLVO Group Trucks Technology for supporting this research. The authors also acknowledge the Conselleria de Innovación, Universidades, Ciencia y Sociedad Digital de la Generalitat Valenciana for partially supporting this research through grant number GV/2020/017.

Nomenclature

ATS	Aftertreatment systems
ASC	Ammonia slip catalyst
BEV	Battery electric vehicles
BMEP	Brake mean effective pressure
BSCO	Brake specific CO emissions
$BSCO_2$	Brake specific CO_2 emissions
BSFC	Brake specific fuel consumption
BSHC	Brake specific HC emissions
BSNOx	Brake specific NOx emissions
BSSoot	Brake specific soot emissions
bTDC	Before fire top dead center
CAD	Crank angle degree
CDC	Conventional diesel combustion
CI	Compression Ignition
CO	Carbon Monoxide
CO2	Carbon Dioxide
CR	Compression ratio
DI	Direct Injection
DMDF	Dual mode dual fuel
DOC	Diesel Oxidation Catalyst
DoE	Design of Experiments
DPF	Diesel particle filter
EHC	Electrically heated catalyst
EMS	Energy management system

EM	Electric motor
EU	European Union
EUVI	European Union version six emission regulation limit
FCEV	Fuel cell vehicles
FHEV	Full hybrid vehicle
HC	Unburned Hydrocarbons
HEV	Hybrid electric vehicle
hp	Horse Power
HP EGR	High pressure Exhaust gas recirculation
ICE	Internal combustion engine
LI-Ion	Litium Ion batteries
LP EGR	Low pressure Exhaust gas recirculation
LTC	Low temperature combustion
MD	Medium Duty
NOx	Nitrogen Oxides
OC	Oxidation Catalyst
OEM	Original equipment manufacturer
P0	Belt alternator starter hybrid powertrain
P1	Parallel hybrid electric vehicle without clutch
P2	Parallel hybrid electric vehicle pre transmission
P3	Parallel hybrid electric vehicle pos transmission
PF	Particle Filter
PFI	Port fuel injection
PHEV	Plug in electric vehicle
PM	particle matter
PN	Particle number
RBC	Rule base control
RCCI	Reactivity Controlled Compression Ignition
rpm	Revolution per minute
SCR	Selective Catalytic Reduction
SI	Spark Ignition
SOC	State of the charge of the battery
ton	Weight in tons (x1000 kg)
TTW	Tank to wheel
WHVC	World Harmonized Vehicle Cycle
WTW	Well to wheel

Appendix

Figure A.1 and Figure A.2 depicts the boundary conditions concerning the state parameters and composition of the exhaust gas that flows through the OC.

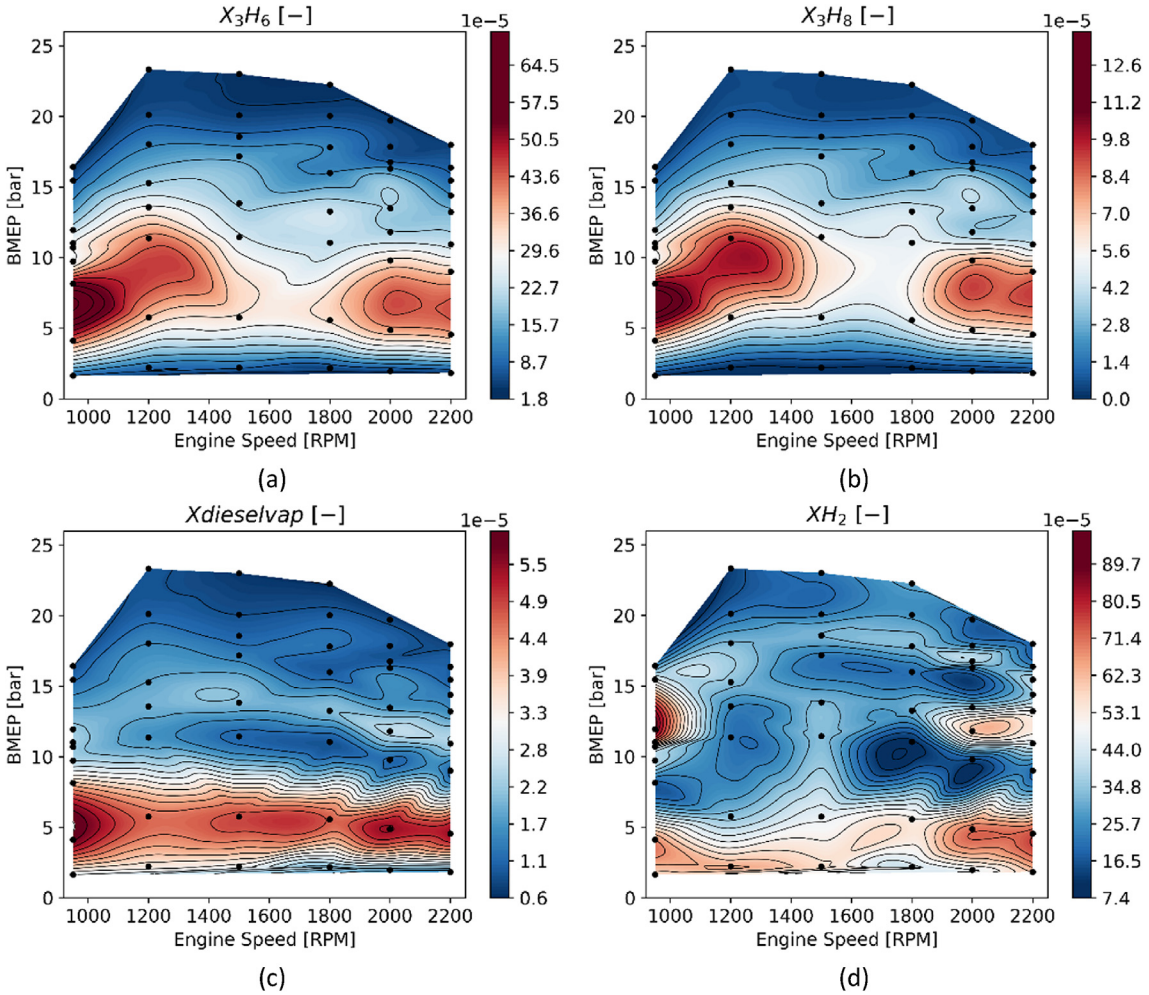

Fig. A1. Engine calibration maps for the RCCI 8 L multi-cylinder Volvo ICE.

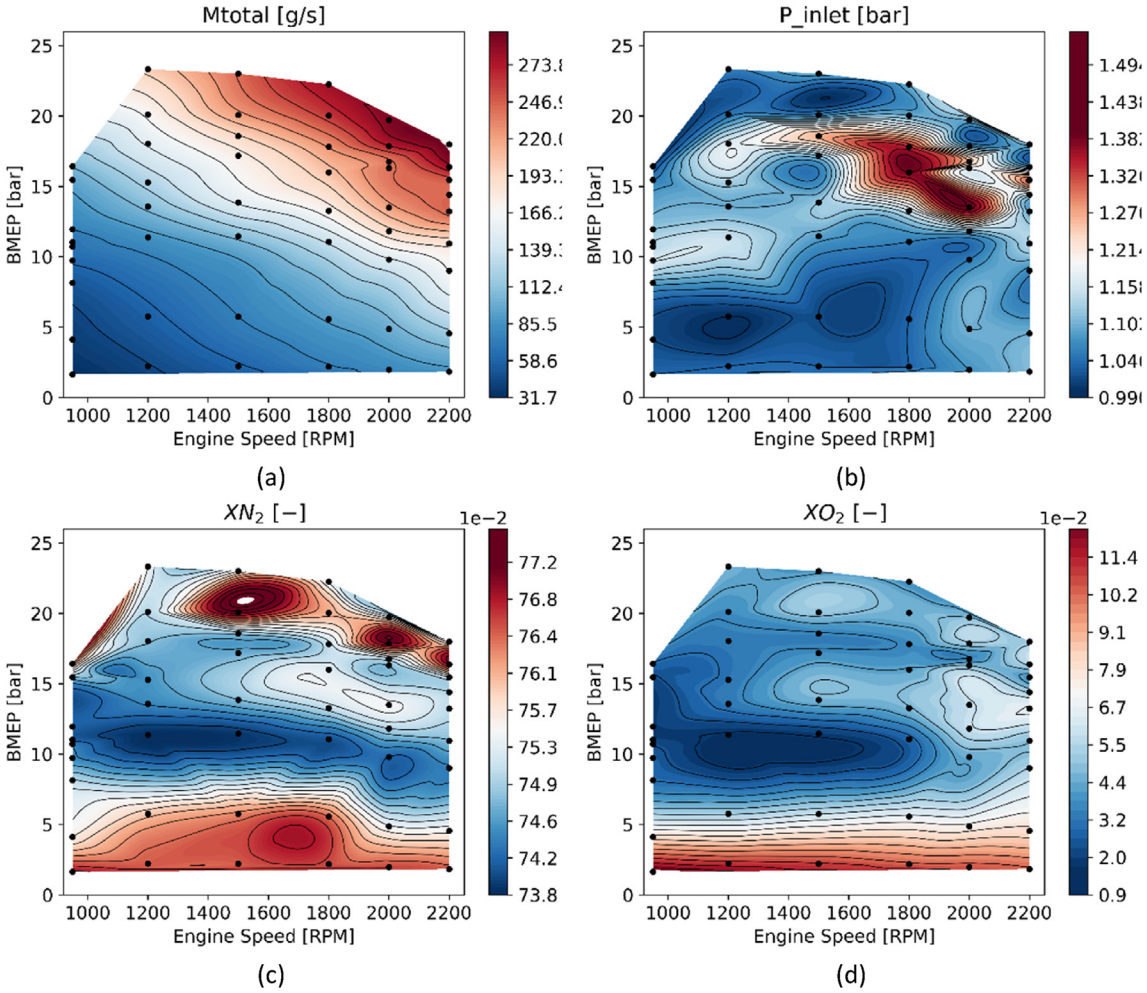

Fig. A2. Engine calibration maps for the RCCI 8 L multi-cylinder Volvo ICE.

Figure A3 shows the methodology used to obtain 3 driving cycles representative of real driving conditions in Paris. The cycles obtained are simulated by SUMO tool, where the open street map is used containing all vehicles information (Figure A3a). The results are visualized in SUMO tool (Figure A3b) where the traffic can be seen online. Figure A4 shows the vehicle speed against time profiles.

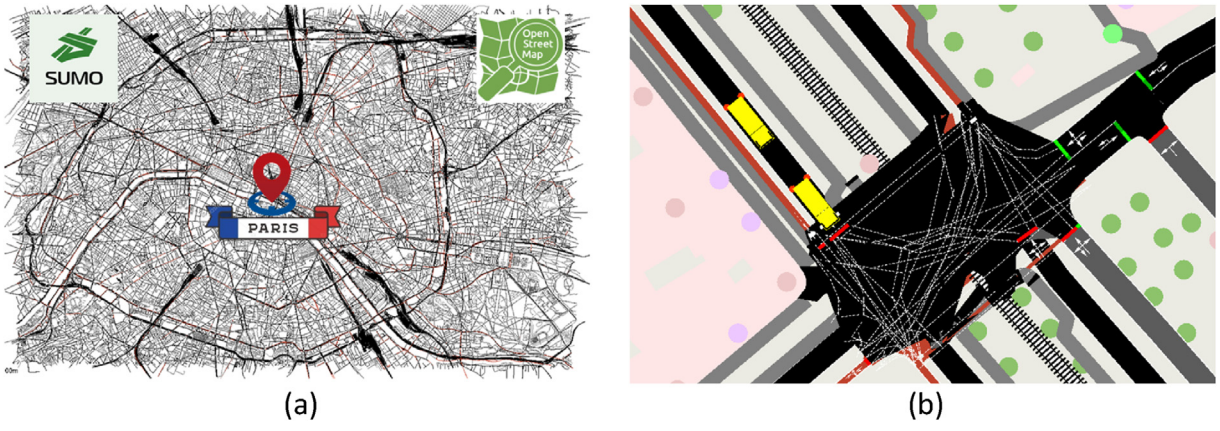

Fig. A3. Open street map of Paris from SUMO platform (a) and traffic track of different truck in SUMO (b).

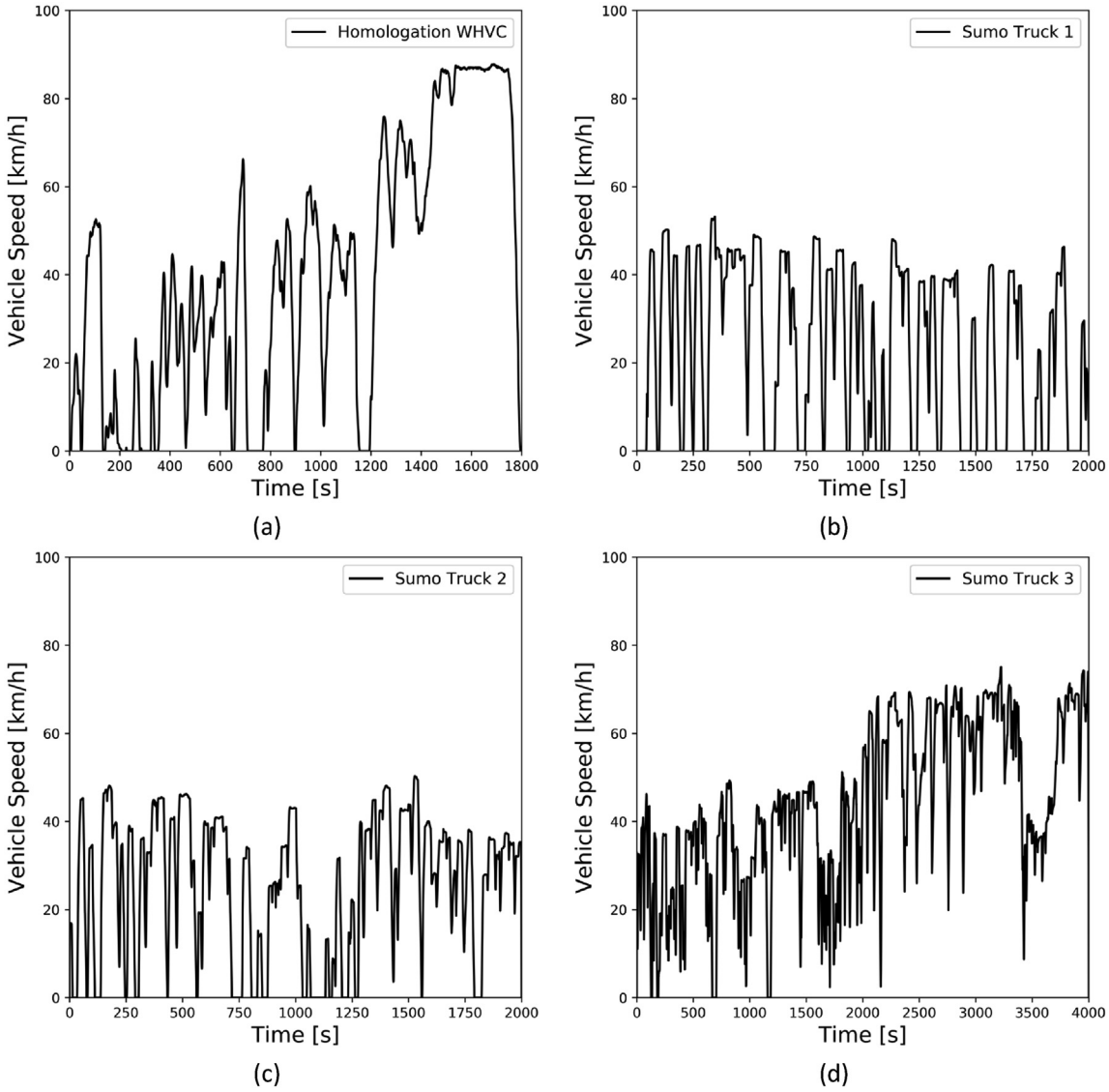

Fig. A4. Driving Cycles, for the 0D vehicle model in WHVC and real routes obtained with SUMO software in Paris centre.

References

[1] Zhu T, Wills RGA, Lot R, Kong X, Yan X. Optimal sizing and sensitivity analysis of a battery-supercapacitor energy storage system for electric vehicles. Energy 2021;221:119851.

[2] Shaobo X, Qiankun Z, Xiaosong H, Liu Y, Xianke L. Battery sizing for plug-in hybrid electric buses considering variable route lengths. Energy 2021;226:120368.

[3] Han W, et al. Study on influencing factors of particle emissions from a RCCI engine with variation of premixing ratio and total cycle energy. Energy 2020;202:117707.

[4] Molina S, García A, Monsalve-Serrano J, Villalta D. Effects of fuel injection parameters on premixed charge compression ignition combustion and emission characteristics in a medium-duty compression ignition diesel engine. Int J Engine Res 2021;22(2):443–55.

[5] Pedrozo VB, May I, Lanzanova TDM, Zhao H. Potential of internal EGR and throttled operation for low load extension of ethanol-diesel dual-fuel reactivity controlled compression ignition combustion on a heavy-duty engine. Fuel 2016;179:391–405.

[6] Benajes J, García A, Monsalve-Serrano J, Lago Sari R. Experimental investigation on the efficiency of a diesel oxidation catalyst in a medium-duty multicylinder RCCI engine. Energy Convers Manag 2018;176(July):1–10.

[7] Zheng Z, Xia M, Liu H, Wang X, Yao M. Experimental study on combustion and emissions of dual fuel RCCI mode fueled with biodiesel/n-butanol, biodiesel/2,5-dimethylfuran and biodiesel/ethanol. Energy 2018;148:824–38.

[8] Benajes J, García A, Monsalve-Serrano J, Martínez-Boggio S. Emissions reduction from passenger cars with RCCI plug-in hybrid electric vehicle technology. Appl Therm Eng Jan. 2020;164(September 2019):114430.

[9] Caliskan H, Mori K. Environmental, enviroeconomic and enhanced thermodynamic analyses of a diesel engine with diesel oxidation catalyst (DOC) and diesel particulate filter (DPF) after treatment systems. Energy 2017;128:128–44.

[10] Sampara CS, Bissett EJ, Chmielewski M. Global kinetics for a commercial diesel oxidation catalyst with two exhaust hydrocarbons. Ind Eng Chem Res 2008;47(2):311–22.

[11] Gao J, Tian G, Sorniotti A, Karci AE, Di Palo R. Review of thermal management of catalytic converters to decrease engine emissions during cold start and warm up. Appl Therm Eng 2019;147(October 2018):177–87.

[12] Yuan R, et al. Modelling and Co-simulation of hybrid vehicles: a thermal management perspective. Appl Therm Eng 2020;180(July):115883.

[13] Horng RF, Chou HM. Effect of input energy on the emission of a motorcycle engine with an electrically heated catalyst in cold-start conditions. Appl Therm Eng 2004;24(14–15):2017–28.

[14] Kang W, Choi B, Jung S, Park S. PM and NOx reduction characteristics of LNT/DPF+SCR/DPF hybrid system. Energy 2018;143:439–47.

[15] Zhang C, Zhang C, Xue L, Li Y. Combustion characteristics and operation range of a RCCI combustion engine fueled with direct injection n-heptane and pipe injection n-butanol. Energy 2017;125:439–48.

[16] Zhou J, Xue S, Xue Y, Liao Y, Liu J, Zhao W. A novel energy management strategy of hybrid electric vehicle via an improved TD3 deep reinforcement learning. Energy 2021;224:120118.

[17] Fontaras G, et al. An experimental evaluation of the methodology proposed for the monitoring and certification of CO2 emissions from heavy-duty

vehicles in Europe. Energy 2016;102:354–64.
[18] Volvo. Volvo FE: product guide. 2017. p. 36.
[19] Benajes J, García A, Monsalve-Serrano J, Boronat V. Dual-fuel combustion for future clean and efficient compression ignition engines. Appl Sci Dec. 2016;7(1):36.
[20] Benajes J, García A, Monsalve-Serrano J, Sari R. Clean and efficient dual-fuel combustion using OMEx as high reactivity fuel: comparison to diesel-gasoline calibration. Energy Convers Manag Jul. 2020;216(March):112953.
[21] García A, Monsalve-Serrano J, Martinez-Boggio S, Gaillard P, Poussin O, Amer AA. Dual fuel combustion and hybrid electric powertrains as potential solution to achieve 2025 emissions targets in medium duty trucks sector. Energy Convers Manag Nov. 2020;224(June):113320.
[22] Benajes J, García A, Monsalve-Serrano J, Martínez-Boggio S. Optimization of the parallel and mild hybrid vehicle platforms operating under conventional and advanced combustion modes. Energy Convers Manag Jun. 2019;190(April):73–90.
[23] Huang Y, et al. A review of power management strategies and component sizing methods for hybrid vehicles. Renew Sustain Energy Rev Nov. 2018;96(April):132–44.
[24] García A, Monsalve-Serrano J, Villalta D, Lago Sari R. Performance of a conventional diesel aftertreatment system used in a medium-duty multi-cylinder dual-mode dual-fuel engine. Energy Convers Manag Mar. 2019;184(February):327–37.
[25] Benajes J, García A, Monsalve-Serrano J, Lago Sari R. Experimental investigation on the efficiency of a diesel oxidation catalyst in a medium-duty multi-cylinder RCCI engine. Energy Convers Manag 2018;176(September):1–10.
[26] García A, Piqueras P, Monsalve-Serrano J, Lago Sari R. Sizing a conventional diesel oxidation catalyst to be used for RCCI combustion under real driving conditions. Appl Therm Eng 2018;140(May):62–72.
[27] Silvis WM. An algorithm for calculating the air/fuel ratio from exhaust emissions. SAE Tech. Pap. 1997;412.
[28] Sosnowski M, Krzywanski J, Scurek R. A fuzzy logic approach for the reduction of mesh-induced error in CFD analysis: a case study of an impinging jet. Entropy 2019;21(11).
[29] Krzywanski J, Czakiert T, Blaszczuk A, Rajczyk R, Muskala W, Nowak W. A generalized model of SO2 emissions from large- and small-scale CFB boilers by artificial neural network approach Part 2. SO2 emissions from large- and pilot-scale CFB boilers in O2/N2, O2/CO2 and O2/RFG combustion atmospheres. Fuel Process Technol 2015;139:73–85.
[30] Krzywanski J, et al. An adaptive neuro-fuzzy model of a re-heat two-stage Adsorption Chiller. Therm Sci 2019;23:S1053–63.
[31] García A, Monsalve-Serrano J, Lago Sari R, Gaillard P. Assessment of a complete truck operating under dual-mode dual-fuel combustion in real life applications: performance and emissions analysis. Appl Energy 2020;279(July):115729.
[32] Della Torre A, Montenegro G, Onorati A, Cerri T. CFD investigation of the impact of electrical heating on the light-off of a diesel oxidation catalyst. SAE Tech. Pap. 2018;2018-April:1–14.
[33] Mianzarasvand F, Shirneshan A, Afrand M. Effect of electrically heated catalytic converter on emission characteristic of a motorcycle engine in cold-start conditions: CFD simulation and kinetic study. Appl Therm Eng 2017;127:453–64.